microbiology research

MDPI

Article

The Presence of an ESBL-Encoding Plasmid Reported During a *Klebsiella pneumoniae* Nosocomial Outbreak in the United Kingdom

Stephen Mark Edward Fordham [1,*], Anna Mantzouratou [1] and Elizabeth Sheridan [1,2]

[1] Department of Life & Environmental Sciences, Talbot Campus Fern Barrow, Bournemouth University, Poole BH12 5BB, UK; amantzouratou@bournemouth.ac.uk (A.M.)
[2] Department of Medical Microbiology, Poole Hospital, University Hospitals Dorset NHS Foundation Trust, Longfleet Road, Poole BH15 2JB, UK
* Correspondence: sfordham@bournemouth.ac.uk

Abstract: An EBSL-encoding plasmid, pESBL-PH, was identified during a nosocomial outbreak of *Klebsiella pneumoniae* ST628 at a United Kingdom general district hospital in 2018. The plasmid from the earliest 2018 *K. pneumoniae* strain discovered during the outbreak was assembled using both Oxford nanopore long reads and illumina short reads, yielding a fully closed plasmid, pESBL-PH-2018. pESBL-PH-2018 was queried against the complete NCBI RefSeq Plasmid Database, comprising 93,823 plasmids, which was downloaded on 16 July 2024. To identify structurally similar plasmids, strict thresholds were applied, including a mash similarity $\geq$0.98. This returned 61 plasmids belonging to 13 unique sequence types (STs) hosts. The plasmids were detected from 13 unique countries, dating from 2012 to 2023. The AMR region of the plasmids varied. Interestingly IS*26*-mediated tandem amplification of resistance genes, including the ESBL gene $bla_{\text{CTX-M-15}}$ was identified in two independent strains, raising their copy number to three. Furthermore, the genomic background of strains carrying a pESBL-PH-2018-like plasmid were analyzed, revealing truncation of the chromosomal *ompK36* porin gene and carbapenem resistance gene carriage on accessory plasmids in 17.85% and 26.78% of strains with a complete chromosome available. This analysis reveals the widespread dissemination of an ESBL-encoding plasmid in a background of resistance-encoding strains, requiring active surveillance.

Keywords: *Klebsiella pneumoniae*; plasmids; ST628; outbreak

Academic Editor: Takayuki Murata

Received: 8 March 2025
Revised: 9 April 2025
Accepted: 18 April 2025
Published: 25 April 2025

Citation: Fordham, S.M.E.; Mantzouratou, A.; Sheridan, E. The Presence of an ESBL-Encoding Plasmid Reported During a *Klebsiella pneumoniae* Nosocomial Outbreak in the United Kingdom. *Microbiol. Res.* **2025**, *16*, 90. https://doi.org/10.3390/microbiolres16050090

1. Introduction

Klebsiella pneumoniae (*K. pneumoniae*) is a major pathogen responsible for healthcare and community-associated infections, including hospital-acquired pneumonia, bloodstream infections (BSIs), urinary tract infections (UTIs), and wound and soft tissue infections. This bacterium's ability to develop resistance to multiple antibiotics presents a significant challenge for effective treatment [1]. In particular, *K. pneumoniae* strains producing extended-spectrum beta-lactamases (ESBLs) are associated with poor clinical outcomes [2]. For example, clinical failure at 7 days was higher in ESBL-producing *K. pneumoniae* UTIs compared to non-ESBL strains [3]. Inadequate empirical antibiotic coverage was a major factor, with appropriate treatment achieved in only 37.7% of ESBL-producing cases, compared to 92.9% for non-ESBL cases [3].

The World Health Organization (WHO) classifies both third-generation cephalosporin-resistant (3GCR) and carbapenem-resistant *K. pneumoniae* as critical threats to human

health [4]. 3GCR *K. pneumoniae* is particularly associated with increased in-hospital mortality, prolonged hospital stays, and higher healthcare costs [4]. Mortality rates are notably high; the 30-day case fatality rate (CFR) for ESBL-producing *K. pneumoniae* BSIs has been reported at 10.6% [5]. In a separate study of 166 patients with BSIs, the overall mortality rate was 43.0% for those infected with ESBL-producing *K. pneumoniae* [6]. In 2019 alone, third-generation cephalosporin-resistant *K. pneumoniae* accounted for approximately 50,100 deaths globally [7].

The most widespread ESBL gene, $bla_{\text{CTX-M-15}}$, has been reported worldwide and is frequently linked to various *K. pneumoniae* clonal lineages, including ST101 [8], ST1427 [9], ST307 [10,11], and ST394 [12]. ESBL genes are commonly located on large, mobile plasmids that can be transferred between species. *K. pneumoniae* serves as a key reservoir for antimicrobial resistance (AMR) genes, effectively acquiring and disseminating these plasmids within its own population and across other Enterobacteriaceae species.

Horizontal transfer of ESBL-encoding plasmids has been documented across several *K. pneumoniae* sequence types (STs) and other Enterobacteriaceae species. A 120 kbp IncFIIK conjugative plasmid encoding $bla_{\text{CTX-M-15}}$, along with seven other AMR genes, was detected in eight isolates from four different *K. pneumoniae* STs (ST416, ST321, ST280, and ST628) and *Enterobacter cloacae* over a one-year surveillance study in a pediatric oncology department in the Czech Republic [13].

In Tanzania, the horizontal transfer of an epidemic IncFII/IncR plasmid (pK012_2) carrying $bla_{\text{CTX-M-15}}$ was detected across 48 different *K. pneumoniae* STs from stool samples collected from both healthy and hospitalized children [14]. This widespread dissemination of a single plasmid across unrelated bacterial clones highlights how F-like conjugation modules contribute to efficient horizontal gene transfer with minimal fitness costs.

In 2018, a clonal outbreak of *K. pneumoniae* ST628 was recorded in a UK district general hospital [15]. The outbreak strain harbored a multi-drug resistant (MDR) plasmid, pESBL-PH encoding 11 AMR genes: *aac(3)-IIe*, *aac(6′)-Ib-cr*, *aph(3″)-Ib*, *aph(6)-Id*, $bla_{\text{CTX-M-15}}$, $bla_{\text{OXA-1}}$, $bla_{\text{TEM-1B}}$, *dfrA14*, *qnrB1*, *sul2*, and *tet(A)*. Antibiotic susceptibility testing (AST) confirmed this plasmid was responsible for resistance to six drug classes, including aminoglycosides, fluoroquinolones, cephalosporins, diaminopyrimidines, sulfonamides, and tetracyclines [15]. Here, we aimed to determine whether the plasmid pESBL-PH-2018, first identified on 3 March 2018 from a UTI patient, was present in other *K. pneumoniae* sequence types (STs). We sought to identify structurally similar plasmids within the complete plasmid database downloaded from NCBI, using stringent thresholds.

2. Materials and Methods

2.1. Genome Assembly and Polishing

The bacterial strain UHD-2018, harboring pESBL-PH-2018, was assembled using hybrid read sets comprising illumina short reads and Oxford Nanopore Technology (ONT) long reads. Initially, raw illumina reads underwent quality control (QC) using fastp v.0.23.4 [16]. Here, low quality reads were discarded, and adapters and low-quality bases were trimmed using default settings. For long-read QC, a minimum length threshold of 6000 bp was applied to the ONT read set. NanoStat v.1.6.0 [17] was used to assess the N50 of the filtered read set, which yielded an N50 of 18,176 bp. Filtlong v.0.2.1 QC was again applied to the filtered read set to remove the worst 10% of the reads using the –keep_percent flag set to 90. Hybrid genome assembly was performed using Trycycler v.0.5.5 [18] using the filtered ONT long read sets using three different assemblers: Flye v.2.9.3-b1797 [19], miniasm/Minipolish v.0.1.2 [20], and Raven v.1.8.3 [21]. A consensus for each cluster generated was performed using Trycycler consensus.

The ONT Medaka polishing tool v.1.11.3 was used to fix any potential remaining errors in the Trycycler ONT long-read assembly. The Medaka model, r941_min_hac_g507, was used, as it best matched the Nanopore pore type and basecaller used for raw FAST5 basecalling. The Trycycler + Medaka assembly was subsequently polished using illumina short reads to fix small-scale errors (single-bp substitutions and indels) using Polypolish v.0.6.0 [22], yielding a FASTA file from the Trycycler + Medaka + Polypolish assembly for the strain UHD-2018.

2.2. Plasmid NCBI RefSeq Database Extraction

The outbreak plasmid, pESBL-PH-2018, was compared against the NCBI RefSeq Plasmid Database using the MinHash Algorithm for fast genome and metagenome distance estimation (Mash) [23] to enable efficient comparisons of large datasets. The complete NCBI RefSeq Plasmid Database, comprising 93,823 plasmids, was downloaded on 16 July 2024.

Mash similarity was determined as 1—mash distance. Pairs of plasmids with mash similarity $\geq$0.98 have previously been considered the same plasmid [24]. Here, we applied this threshold, in addition to the number of shared hashes, to return similar completely assembled plasmids from the complete NCBI RefSeq database. Plasmids were filtered for both a shared hash ratio of 0.9 and a mash similarity $\geq$0.98, yielding plasmids with >91% coverage and >99.8% identity against pESBL-PH-2018. Using this strict threshold, highly similar plasmids can be captured, and we used this definition to define a pESBL-PH-2018-like plasmid. The accession number for each plasmid was used to retrieve the following information from NCBI: plasmid length, geographical source isolation, host strain, host disease, and host source.

2.3. Plasmid Antimicrobial Resistance (AMR) Genes, Stress-Related Genes and In Silico Conjugation Detection

AMR, virulence and stress-associated genes were annotated using the AMRFinderPlus 2024-05-02.2 database [25]. Whole genome annotation of the assembled strain UHD-2018, including pESBL-PH-2018, was performed using Bakta v.1.9.3 [26] with the full database version, updated on 16 July 2024. In silico plasmid conjugative capacity was predicted using Plascard [27] via the presence of a mobilization of plasmids (F) (MOBF) region, a type IV coupling protein (T4CP), and a type IV secretion system (T4SS).

2.4. Single Nucleotide Polymorphisms (SNPs) Detection Among Recombination-Filtered pESBL-PH-2018-like Plasmids

Snippy v.4.6.0 (https://github.com/tseemann/snippy), accessed 4 July 2024, was used to determine single-nucleotide polymorphisms (SNPs) between the annotated pESBL-PH-2018 plasmid and similar plasmids retrieved via the Mash search criteria described above. The reference Genbank file pESBL-PH-2018.gbff, output via the Bakta annotation tool, was set at the reference sequence. To determine the number of SNPs between the core genetic loci of pESBL-PH-2018 and other plasmids, predicted regions of recombination in other plasmids were removed using Gubbins v.3.3.1 [28]. The output file, recombination_predictions.gff, was used to determine recombination regions (see Supplementary File S1).

Additionally, a strict threshold was applied to determine the relatedness between pESBL-PH-2018 and the query plasmids. An SNP count of fewer than 15 per 100 kbp was used to determine high similarity between the plasmids and to infer likely horizontal plasmid transfer, as previously determined [29]. To achieve this, recombination regions were removed from the total query plasmid length. Core SNPs were then divided by the query plasmid length without the recombinant region(s). This yielded an SNP rate per

recombination-free plasmid sequence, which was converted to provide an SNP rate per 100,000 bp.

2.5. Plasmid Detection in Phylogenetically Distinct Bacterial Clones

The host bacterial strain from each plasmid was downloaded from NCBI. A recombination-free phylogenetic tree was constructed to confirm that strains harboring a pESBL-PH-2018 plasmid belong to phylogenetically distinct clones. Snippy-core v.4.6.0 (https://github.com/tseemann/snippy, accessed on 4 July 2024) was used to create an alignment between all host chromosomal FASTA files. Gubbins v.3.3.1 [28] was then run to create a recombination-filtered tree using RAxML, generating a maximum-likelihood (ML) phylogenetic tree using 100 rounds of bootstrapping replicates. FigTree v1.4.4 was used to visualize the resulting phylogenetic tree.

2.6. Core Backbone Evaluation

The core genome from plasmids derived from phylogenetically diverse host strains were evaluated to determine the core backbone and shared gene content. Roary v.3.12.0 [30] was used with the following parameters:

roary -e –maftt, -p 8 *.gff

3. Results

3.1. Plasmid Similarity Against pESBL-PH-2018: An Overview

The strict search criteria yielded 61 similar plasmids. The similarity between the query plasmids and the reference pESBL-PH-2018 was compared using a series of methods. The Mash distance metric, based on the Jaccard index of *k*-mer sketches (subsequences of length *k*) was initially used to assess plasmid similarity (Supplementary File S1). A mean Mash similarity (1—Mash distance) of 0.9992 was recorded, with a standard deviation (σ) of 0.0007 and an interquartile range (IQR) of 0.9988–0.999. Additionally, the number of shared hashes was assessed as a ratio. Across the collection of 61 plasmids samples, the hash ratio ranged from 0.902 to 1.00 (mean: 0.968, IQR: 0.954–0.998, median: 0.969, σ: 0.029).

The nucleotide coverage and identity were also compared between each of the 61 query plasmids and the reference, pESBL-PH-2018. BLASTn (version 2.14.1) coverage for the plasmids against pESBL-PH-2018 ranged from 91 to 100% (mean: 97.82%, IQR: 97–100%, median: 98.0%, σ: 2.34). The BLASTn identity of the query plasmids against pESBL-PH-2018 was high; range 99.87–100.00% (mean: 99.99%, IQR: 99.99–100.00%, σ: 0.019). Finally, the length of the plasmids was assessed. The 61 query plasmids had a mean length of 244,365 bp. When each plasmid was compared against the reference length of pESBL-PH-2018, 247, 179 bp, the IQR for plasmid length was between 97.56–99.99% of the length of pESBL-PH-2018. Taken together, the high Mash similarity, shared hashes, high coverage, and nucleotide identity, combined with a similar length, suggest that all 61 plasmids are highly similar to pESBL-PH-2018.

3.2. Identification of pESBL-PH-2018-like Plasmids: Host Strain and Isolation Source

The host bacterium strain harboring each of the query plasmids were downloaded from the NCBI nucleotide database. Across the collection of 57 plasmid samples where a host bacterium ST designation was assigned, 13 unique sequence types (STs) were identified. The pESBL-PH-2018-like plasmid was detected most frequently in *K. pneumoniae* ST307 (n = 21/57, 36.84%). Furthermore, pESBL-PH-2018-like plasmids were found in five STs, where the ST was identified three or more times: ST628 (n = 9/57, 15.78%), ST323 (n = 8/57, 14.03%), ST29 (n = 5/57, 8.77%), ST405 (n = 3/57, 5.26%), and ST11 (n = 3/57, 5.26%). In addition, the pESBL-PH-2018-like plasmid was identified in seven other STs: ST617, -280,

-479, -6265, -2856, and ST584, respectively (Figure 1A). Across 60 samples where a host strain species was recorded, the pESBL-PH-2018 like plasmid was predominately detected in *K. pneumoniae* (n = 57/60, 95%). Separately, three similar plasmids were detected in two different genera, while a single plasmid was detected in different species: plasmid P1 was detected in a *Klebsiella oxytoca* strain; plasmid 2, in KPN029 *Klebsiella variicola* ST347; and pCUVET16-321.1, in an *Escherichia coli* ST479 strain. Together, these results suggest different *Klebsiella* genera and other species may be receptive carriers for pESBL-PH-2018-like plasmids.

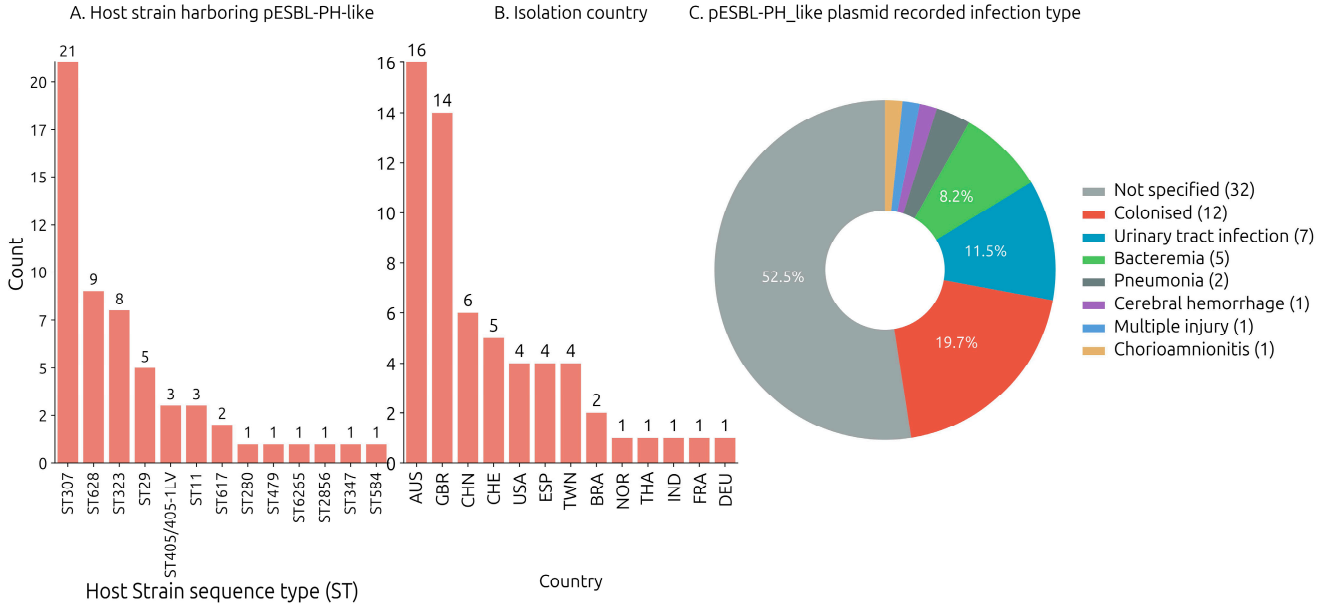

Figure 1. Plasmid host strain, country, infection source, and timeline identification. (**A**). Host strain ST designation. (**B**). Country of isolation accessed via available Biosample data from NCBI. (**C**). Infection type assignment determined according to metadata available via Biosample data from NCBI.

The pESBL-PH-2018-like plasmid was identified in 13 unique countries between 2012 and 2023 (Figure 1B). The available Biosample data from NCBI indicated the plasmid (including pESBL-PH-2018) was most often found in Australia (26.22%, n = 16/60), the United Kingdom (22.95%, n = 14/60), and China (9.83%, n = 6/60). Separately, the plasmid was identified ≥4 times in Switzerland, USA, Spain, and Taiwan (Figure 1B). Available Biosample data also indicated the pESBL-PH-2018-like plasmids (including pESBL-PH-2018) were identified from a range of infection types including urinary tract infections (11.3%, n = 7), bacteremia (8.1%, n = 5), pneumonia (3.2%, n = 2), cerebral hemorrhage (1.6%, n = 1), acquisition from wounds via injuries (1.6%, n = 1), and chorioamnionitis (1.6%, n = 1), respectively (Figure 1C).

Interestingly, among the 61 query plasmids similar to pESBL-PH-2018, the majority, n = 57/61 (93.44%), were identified from human hosts. Forty-seven of these samples had a clinical source isolation (Supplementary File S1); the remaining 10 samples lacked data on their isolation source. In hospital settings, high and frequent use of antibiotics can create strong selective pressure favoring bacteria that carry MDR plasmids.

Four samples, however, n = 4/61 (6.55%), were identified from the environment and/or non-human hosts, including one sample collected from stream water (pEW1149-1), one sample from river water (pEW758-CTX-M-15), another sample from milk in an environmental sample (pKP102-1), while the pESBL-PH-2018-like plasmid pCUVET16-321.1, was identified in a urine sample from a ST479 *E. coli* sample obtained from a dog.

These results suggest that the pESBL-PH-2018-like plasmid can be found beyond the confines of clinical settings.

The collection dates of plasmids with a recorded year, month, and day were investigated. Plasmids similar to pESBL-PH-2018 were collected from 16 January 2012 in Barcelona, Spain (pKp589-231, accession: CP028817.1) through to 17 January 2023 in the USA (2023CK-0011, plasmid unnamed, accession: CP131947.1). The interval between the detection of these two plasmids is 11 years and 4 days. Similar plasmids were detected from 25% (n = 11) of the samples with a collection date in 2014, while 20.45% (n = 9) were collected in 2018; however, ≥3 similar plasmids were recorded in 2014, 2017, 2018, 2020, and 2022 (Figure 2). These results reveal a consistent presence of ESBL-encoding plasmids similar to pESBL-PH-2018. A recombination-filtered phylogenetic tree of host bacterial strains revealed that the plasmids were carried by distinct bacterial clones. Across these clones, evidence of expansion of the host strain with the plasmid is seen (Figure 3).

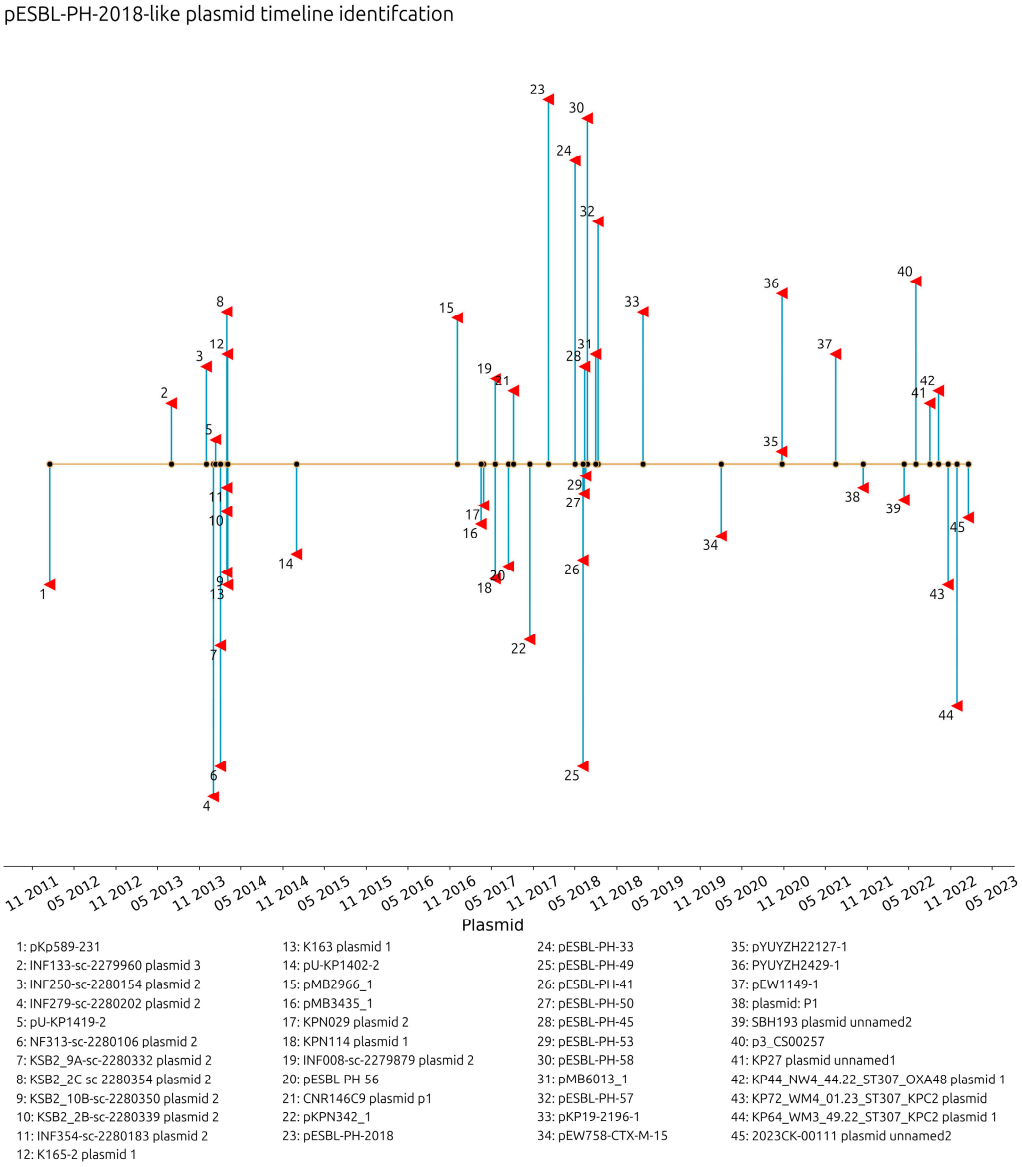

Figure 2. The identification of similar plasmids to pESBL-PH-2018 plotted as per their discovery. Each plasmid name matches the numbered key. Plasmid metadata is available in Supplementary File S1.

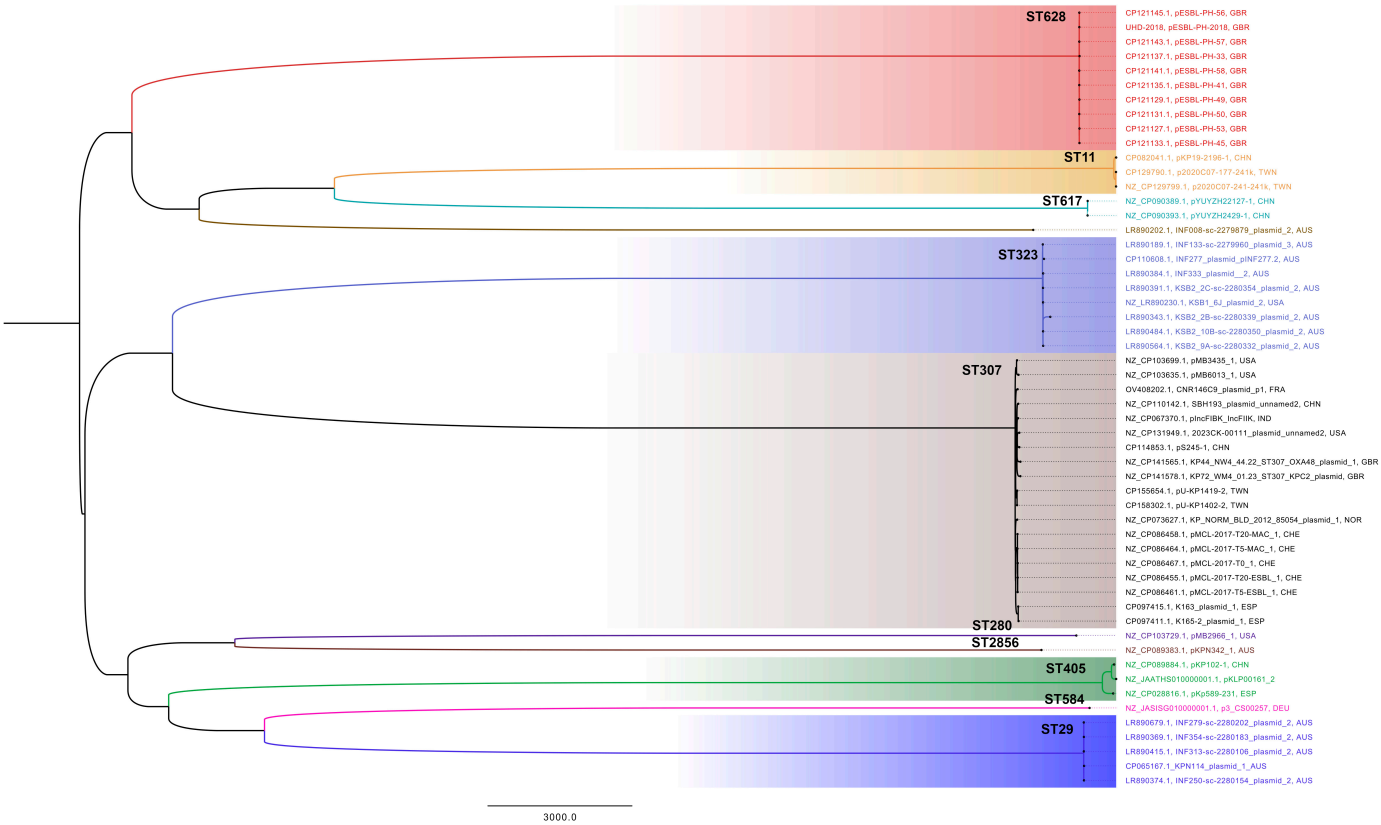

Figure 3. Host strain carrying plasmids similar to pESBL-PH-2018, colored according to their clade. Plasmid accession, name, and country source are listed at the tips of each branch. The recombination-filtered phylogenetic tree was constructed using RAxML, generating a maximum-likelihood (ML) phylogenetic tree using 100 rounds of bootstrapping replicates. FigTree v1.4.4 was used to visualize the resulting phylogenetic tree. The scale refers to the number of SNPs.

3.3. Single Nucleotide Polymorphism Analysis

Single nucleotide polymorphisms (SNPs) between pESBL-PH-2018 and the query plasmids were investigated to provide high-resolution analysis of their relatedness. SNP analysis was performed on recombinant-removed query plasmids. Across the selection of plasmids, an average of 4.95 SNPs were detected (range: 0–16, IQR: 3–6); 93.44% (n = 57/61) of plasmids had an SNP count $\leq$10, while 65.5% (n = 40/61) had an SNP count $\leq$ 5. With the exception of CNR146C9 plasmid 1 and p3_CS00257 each of which had a recombination region of 6757 bp and 17,782 bp, respectively, a mean recombinant region of 531 bp was identified (range: 0–2396 bp), which, on average, only constituted 0.22% of their overall plasmid length, revealing that the plasmids shared large stretches of identical sequences. Across all plasmid samples, an average of 1.95 SNPs/100 kb was identified, suggesting that the plasmids were closely related to pESBL-PH-2018 (Figure 4, Supplementary File S1).

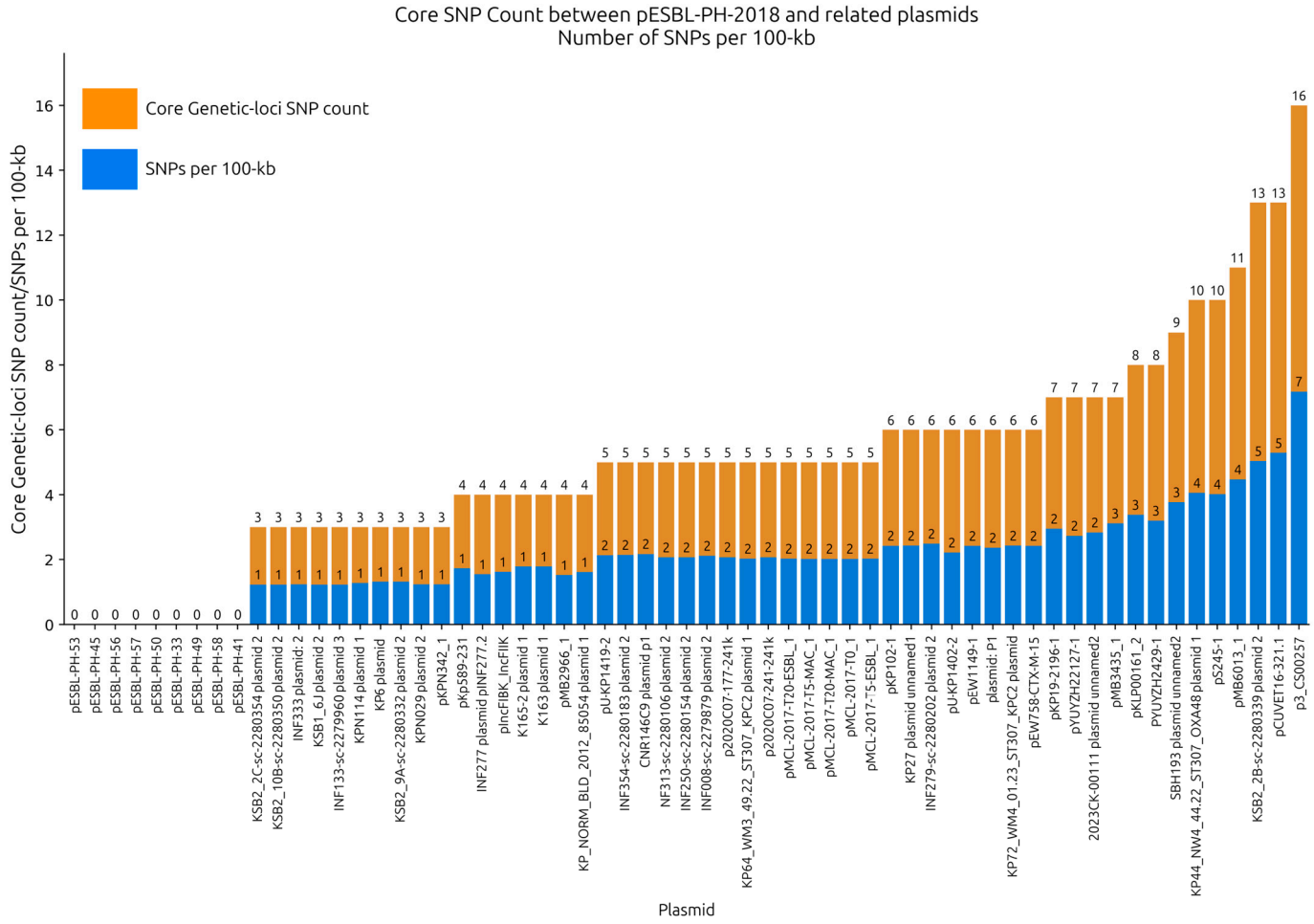

Figure 4. SNP distance between pESBL-PH-2018 and query plasmids. The core genetic loci between query plasmids and pESBL-PH-2018 were compared to determine the number of SNPs to use as a proxy of plasmid relatedness (orange). Plasmid relatedness was normalized to the number of SNPs/100 kb in core genomic loci (blue).

3.4. Core Genome Analysis

The core genome analysis was performed on 12 plasmids (Table 1) from *K. pneumoniae* strains, representing 12 unique sequence types (STs). This approach aimed to identify conserved genetic elements constituting the plasmid backbone, which are essential for plasmid maintenance, stability, and potential conjugative transfer across diverse host strains. A total of 210 genes were shared across all plasmids, with a combined nucleotide length of 182,216 bp. Additionally, 90.9% of genes (n = 281/309) were classified as either core genes (present in 99–100% of plasmids) or shell genes (present in 15–95% of plasmids). Only 9.1% of genes (28/309) were considered cloud or accessory genes, highlighting the substantial conservation of core genetic elements across diverse host strains. The core backbone and shared gene content are visualized for representative STs in Figure 5.

While the plasmid analysis initially identified 13 unique host strain STs, the plasmid pMB2966_1 from *K. pneumoniae* ST280 was excluded from the core genome analysis due to the presence of a segmental duplication. This duplication encompassed several AMR genes, including *sul2*, *aph(3″)-Ib*, *aph(6)-Id*, $bla_{\text{TEM-1}}$, and $bla_{\text{CTX-M-15}}$. Including this plasmid in the analysis would have skewed the results by artificially inflating the number of genes classified as core, thereby distorting the overall structure of the core genome.

Table 1. Plasmid samples used for core genome analysis.

Plasmid	Host ST	Host Species
KPN029 plasmid 2	ST347	*K. variicola*
KP_NORM_BLD_2012_85054 plasmid 1	ST307	*K. pneumoniae*
pKP19-2196-1	ST11	*K. pneumoniae*
pKPN342_1	ST2856	*K. pneumoniae*
pKP102-1	ST405	*K. pneumoniae*
pYUYZH22127-1	ST617	*K. pneumoniae*
SBH193 plasmid 2	ST6265	*K. pneumoniae*
pESBL-PH-56	ST628	*K. pneumoniae*
pCUVET16-321.1	ST479	*E. coli*
P3_CS00257	ST584	*K. pneumoniae*
INF250-sc-2280154 plasmid 2	ST29	*K. pneumoniae*
KSB2_2C-sc-2280354 plasmid 2	ST323	*K. pneumoniae*

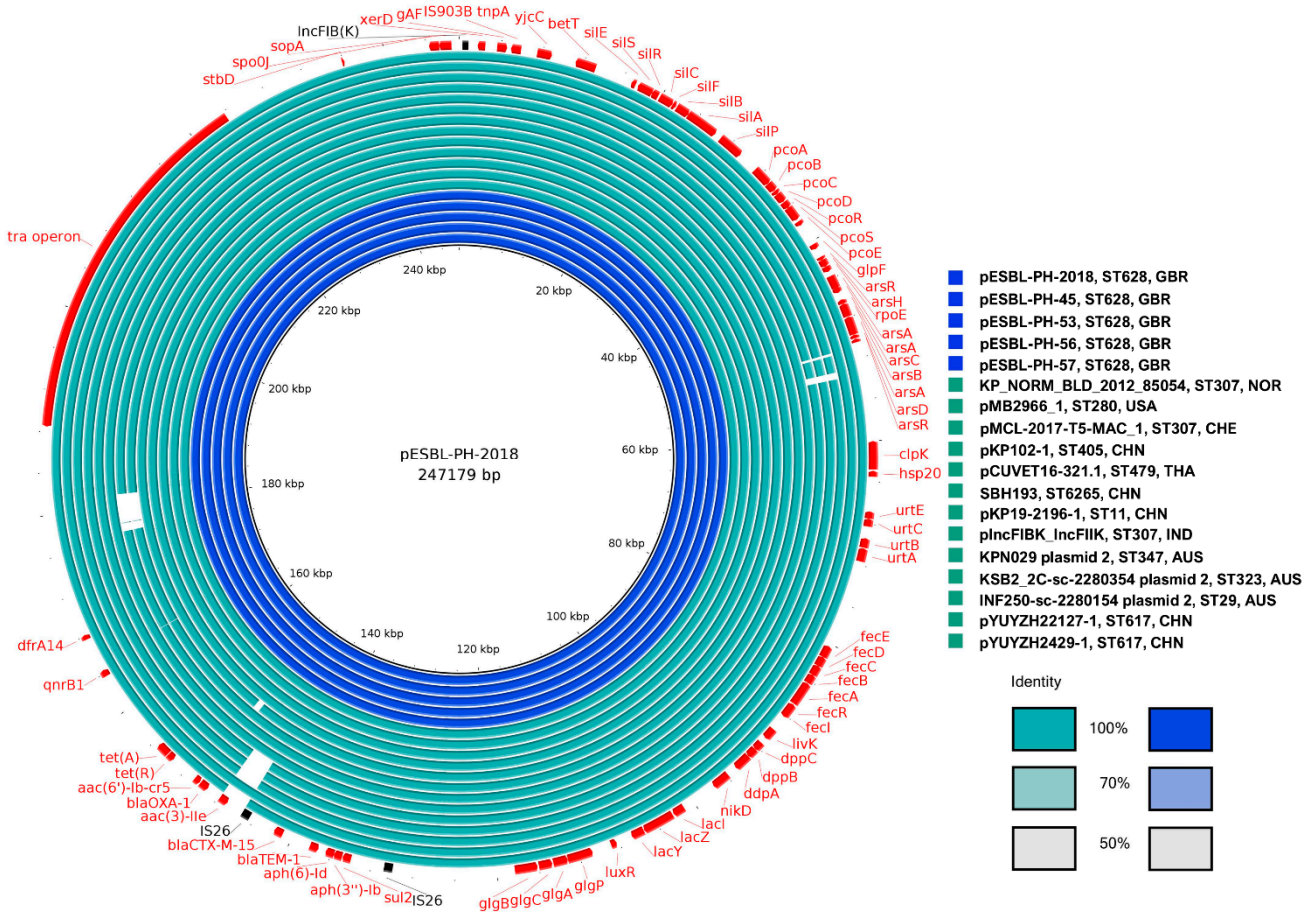

Figure 5. Comparison of pESBL-PH-2018 with similar plasmids. Each plasmid is represented by a circular ring, ordered from the innermost (top of the key) to the outermost (bottom of the key). The plasmid visual comparison was performed using the BLAST Ring Image Generator (BRIG) [31]. The comparison was performed across a range of plasmids identified from 11 unique hosts. The genes are indicated on the outer ring in red with their direction of transcription indicated by an arrowhead.

The exclusion of pMB2966_1 ensured that the identified core genome reflected genuinely conserved elements, rather than artifacts arising from gene duplication or rear-

rangement. Interestingly, despite differences in AMR gene content, all plasmids shared several stress-related genes with 100% identity and coverage, including silver (*silS*, *silR*, *silC*), copper (*pcoABCR*), and arsenic (*arsABCR*) heavy metal resistance genes, alongside the heat shock gene *hsp20*. Furthermore, all plasmids were classified as IncFIB(K) and were predicted to be conjugative, possessing essential components for horizontal gene transfer, such as a relaxase, T4SS, and T4CP.

3.5. AMR Variants

From the collection of plasmids including pESBL-PH-2018, 54.8% (n = 34/62) carried exactly one copy of the 11 AMR genes: *aph(3″)-Ib*, *aph(6)-Id*, $bla_{\text{TEM-1B}}$, $bla_{\text{CTX-M-15}}$, *aac(3)-IIe*, $bla_{\text{OXA-1}}$, *aac(6′)-Ib-cr*, *tet(A)*, *qnrB1*, *dfrA14* and *sul2*. Plasmids pMB2966_1 and pMB6013_1 carried multiple copies of these genes, including either 2 or 3 copies each of the ESBL gene, $bla_{\text{CTX-M-15}}$, respectively (Figure 6). In total, 58% of the plasmids carried either one or more of the total complement of 11 AMR genes carried by pESBL-PH-2018. Notably, a common variant, which lacked only *aac(3)-IIe* was detected in 24.19% (n = 15/62) of samples. From these 15 samples, 13 samples were identified from Australia, confirming that the *aac(3)-IIe* aminoglycoside gene was commonly missing from plasmids related to pESBL-PH-2018 sourced from Australia.

Although similar plasmids to pESBL-PH-2018 were detected, a number of variants with different numbers of the same AMR genes were observed. The aminoglycoside resistance gene, *aac(3)-IIe*, was absent from a number of plasmids. In comparison to pESBL-PH-2018, plasmid pKPN342_1 (accession: CP089384.1), an AMR variant lacking *aac(3)-IIe*, had a deletion of 3420 bp, including *aac(3)-IIe* and a complete copy of IS*26* located between two inverted sequences (Figure 6). A similar deletion of 2600 bp encompassing *aac(3)-IIe* was identified in plasmid KBS2_10B (accession: LR8900485.1). However, in this plasmid, both copies of the IS*26* between *aac(3)-IIe* were retained.

Separately, KP_NORM_BLD_2012_85054 plasmid 1 (accession: CP073628.1) from *K. pneumoniae* ST307 encoded the TEM variant, $bla_{\text{TEM-206}}$. This variant was due to an SNP at nucleotide position 25, resulting in a missense variant, whereby the non-polar amino acid alanine was replaced by the polar amino acid threonine at amino acid position 9.

Variants with two copies of several AMR genes, including the ESBL gene, $bla_{\text{CTX-M-15}}$, were identified. pMB2966_1 had two copies each of the following genes: *sul2*, *aph(3″)-Ib*, *aph(6)-Id*, $bla_{\text{TEM-1}}$, and $bla_{\text{CTX-M-15}}$, respectively. In pESBL-PH-2018, these AMR genes are present within a 15,310 bp IS*26* pseudo-compound transposon (PCT). However, in pMB2966_1, a segmental duplication (mobilization to another genomic context) of a 16,374 bp region, including an inverted copy, carrying these genes was observed. Both regions carrying these AMR genes shared 12,212 bp with the IS*26* PCT from pESBL-PH-2018, but both segments lacked IS*26* insertion sequences bracketing the 5 AMR genes, confirming that the duplication of these genes did not occur due to an IS*26*-mediated translocatable unit (TU) amplification. Additionally, plasmid 2 (accession: LR890344.1) from *K. pneumoniae* ST323, obtained from a rectal swab, had a segmental duplication of 10.98 kb, including the AMR gene, *dfrA14*. Similar to pMB2966_1, the second segmental copy lacked IS*26* elements on either side of the duplication.

For plasmid pU-KP1402-2, two copies each of $bla_{\text{CTX-M-15}}$, *aac(3)-IIe*, $bla_{\text{OXA-1}}$, *aac(6′)-Ib-cr*, *tet(A)*, and *qnrB1* were identified. Here, $bla_{\text{CTX-M-15}}$ and *aac(3)-IIe* were duplicated as an additional inverted copy associated with a single copy of IS*26* *tnpA26*. Another inverted duplication was also observed for $bla_{\text{OXA-1}}$ and *aac(6′)-Ib-cr*, with both copies having inwardly facing *tnpA26* transposases. Interestingly, both *tet(A)* and *qnrB1* were also duplicated.

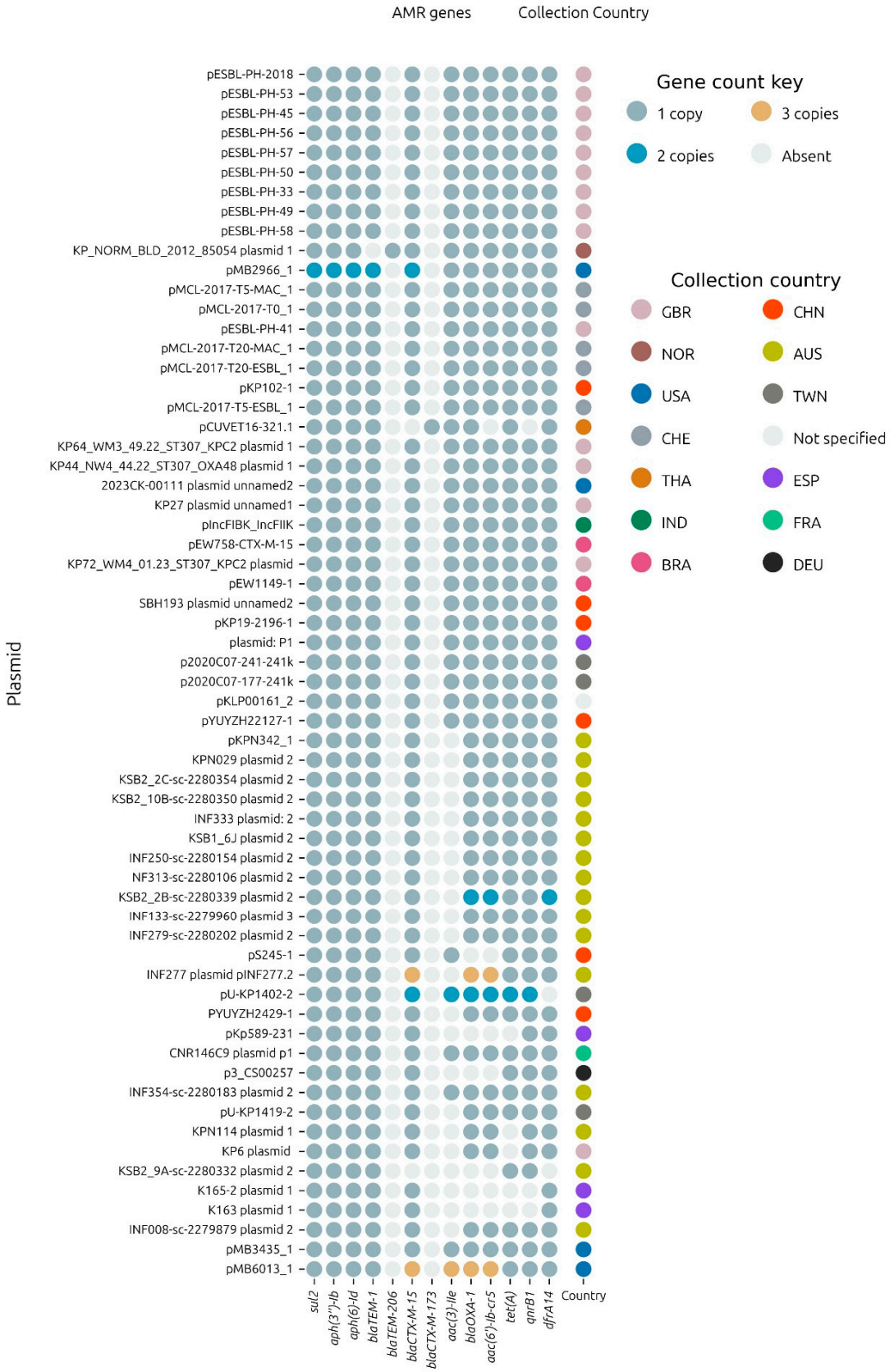

Figure 6. Antimicrobial resistance genes present among plasmids similar to pESBL-PH-2018. AMR genes are marked as absent (white) and according to their copy number: 1 (grey), 2 (blue), and three (light brown). Countries are indicated according to their IBAN country code and color-coded accordingly.

Two plasmid variants, pMB6013_1 (accession: CP103636.1) and pINF277.2 (accession: CP110610.1), with a copy number of three for the ESBL gene *bla*$_{\text{CTX-M-15}}$ and other AMR genes were also investigated. Here, IS*26*-TU tandem amplification was identified. While pESBL-PH-2018 was similar to pMB6013_1, the AMR region varied. Relative to pESBL-PH-2018, a transposase gene and the ESBL gene *bla*$_{\text{CTX-M-15}}$ are inverted. This inversion lies upstream of an IS*26 tnpA26* and downstream of an inverted region carrying three AMR genes, *aac(6′)-Ib-cr*, *bla*$_{\text{OXA-1}}$, and *aac(3)-IIe*. Together, this forms a section of four AMR genes bracketed by IS*26 tnpA26 on* each side (Figure 7). This region was duplicated, generating three tandem copies of these AMR genes. The AMR tandem repeat is 11,009 bp, measured from the inverted repeat left (IRL) of IS*26* to the shared region of the Tn3 transposase fragment (marked boxes Figure 7). The genomic organization indicates IS*26*-mediated TU amplification may have created the tandem array.

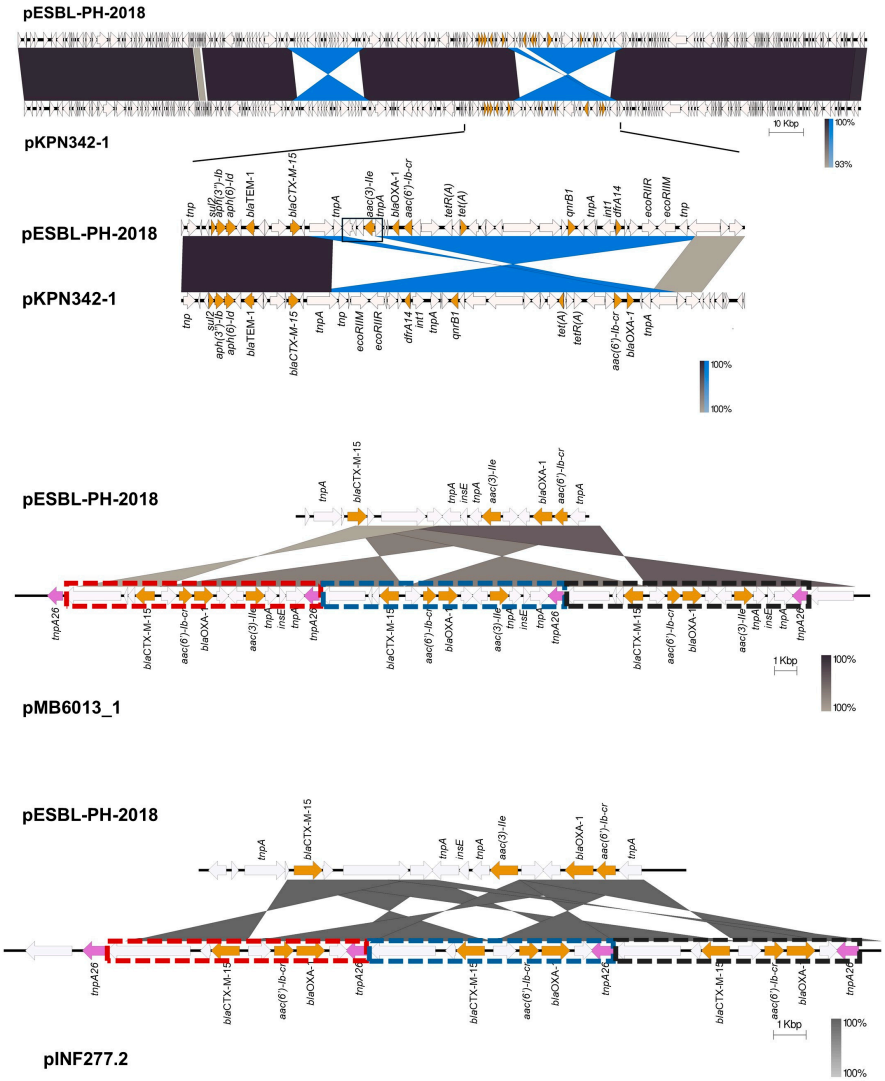

Figure 7. Comparison between the the AMR region of pESBL-PH-2018 and similar plasmids. Top: likely IS*26*-medatied deletion of the aminoglycoside resistance gene, *aac(3)-IIe*. Middle: for pMB6013_1 (accession: CP103636.1), isolated from a *K. pneumoniae* ST307 strain from a patient with bacteremia, three tandem copies of the AMR genes were present in a 11,009 bp array: *bla*$_{\text{CTX-M-15}}$, *aac(6′)-Ib-cr*, *bla*$_{\text{OXA-1}}$, *aac(3)-IIe*. Bottom: For pINF277.2, IS*26*-mediated TU amplification of a 7559 bp region carrying the AMR genes *bla*$_{\text{CTX-M-15}}$, *aac(6′)-Ib-cr*, *bla*$_{\text{OXA-1}}$, and *aac(3)-IIe* was present in a tandem array, as indicated by the three colored bordered boxes. Tandem repeats were measured from the inverted repeat left (IRL) of IS*26* to the end of the shared Tn3 family transposase fragment, represented in each tandem array as the longest white arrow (at the left end of each bordered box).

Separately, pINF277.2 from *K. pneumoniae* ST323, isolated from a bronchoalveolar lavage (BAL) sample from a patient with pneumonia, also had a similar IS*26*-mediated TU amplification for the three AMR genes: $bla_{\text{CTX-M-15}}$, *aac(6′)-Ib-cr*, and $bla_{\text{OXA-1}}$. Relative to pESBL-PH-2018, $bla_{\text{CTX-M-15}}$ is inverted and lies upstream of a shared IS*26 tnpA26* transposase. The AMR region from pESBL-PH-2018, including *aac(6′)-Ib-cr*, $bla_{\text{OXA-1}}$ and *tnpA26,* is inverted and located downstream of $bla_{\text{CTX-M-15}}$ (Figure 7). This region in pINF277.2, bracketed by *tnpA26*, is duplicated three times, increasing the copy number for each of these genes to three. The IS*26*-mediated TU tandem array here was 7559 bp (marked boxes, Figure 7).

3.6. Host Strain Background

The host strain background for 56 strains with a complete chromosome was investigated for AMR, virulence, and stress-associated factors. In particular, gene mutations associated with carbapenem resistance were analyzed. The pESBL-PH-2018-like plasmid was present in a background associated with carbapenem resistance mechanisms. Notably, 26.78% (n = 15/56) of the strains encoded a carbapenem resistance gene on an accessory plasmid in addition to carrying a pESBL-PH-2018-like plasmid (Figure 8). In addition, 17.85% (n = 10/56) of the strains had a truncation in the outer membrane porin gene, *ompK36*, disruptions of which can reduce the permeability of the outer membrane to carbapenems. Porin truncations were present in four strains, which also carried a carbapenemase gene on an accessory plasmid (Figure 8). Three strains carried the *ompK36* variant, *ompK36_D135DGD*, associated with porin constriction mediated by the di-amino acid (Gly115-Asp116) insertion into loop 3 of the OmpK36 porin [32]. This change has been associated with restricted access to carbapenems into the host cell. Two of these variants were found, in addition to carbapenem resistance genes present on separate plasmids (Figure 8, Supplementary File S2).

Colistin resistance associated gene variants were also detected in 14.28% (n=8/56) strains. Here, 5 strains carried the *pmrB* gene variant: *pmrB_R256G*, 1 carried the *pmrB_Y358N* variant, while 2 strains carried both the *pmrB_T157P* alongside a gene truncation in *mgrB*. Such changes have been associated with constitutive activation of the two-component system, PmrA-PmrB, leading to a reduction in the negative charge of the bacterial lipopolysaccharide (LPS) present on the bacterial outer membrane. The reduction in negative charge decreases the binding affinity of colistin (a cationic peptide), leading to colistin resistance.

Notably, a large proportion, 92.85% (n = 52/56), of the isolates were predicted to encode the chromosomal fosfomycin resistance gene, *fosA*. In addition, a number of predicted quinoline resistance-inducing mutations impacting either DNA gyrase or topoisomerase IV were detected. In particular, all representative ST11 and ST307 isolates encoded the *gyrA* S83I and *parC* S80I double mutations. A proportion of strains, 14.28% (n = 8/56), also encoded the virulence-associated YbtPQ ABC transporter, a key transporter system involved in both iron acquisition during infection and broad export of antimicrobials. Taken together, AMR, virulence and stress-associated typing of the chromosomes and plasmids co-present with the pESBL-PH-2018-like plasmid reveal a genomic background associated with genes conferring resistance to critical and last-resort antimicrobials, such as carbapenems and colistin, in addition to the six classes of AMR resistance conferred by pESBL-PH-2018.

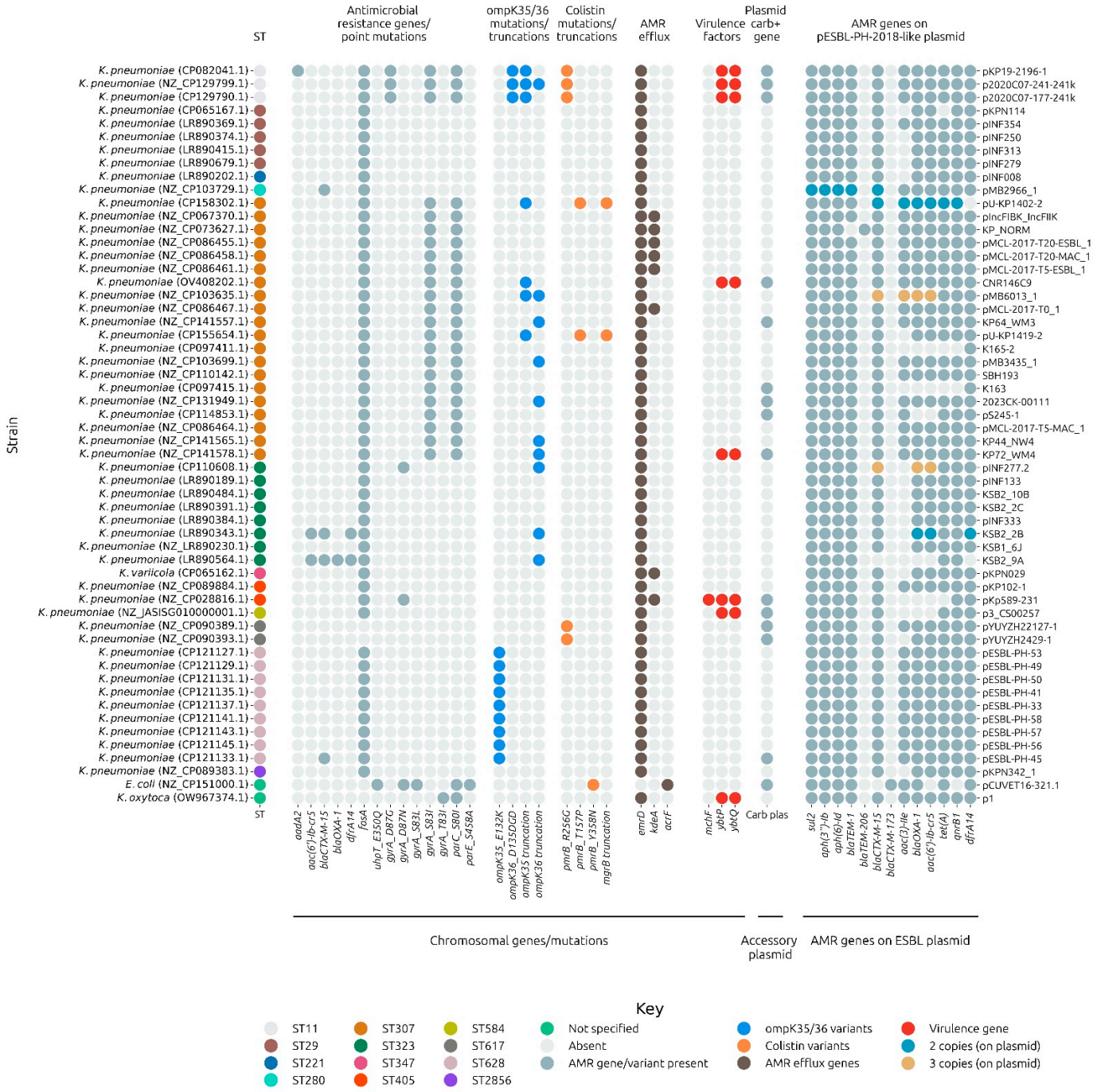

Figure 8. AMR genes/point mutations, porins, and virulence-associated factors among strains carrying pESBL-PH-2018-like plasmids. Strains carrying a pESBL-PH-2018-like plasmid are listed on the left *y*-axis according to their ST; the pESBL-PH-2018-like plasmid carried by the strain is indicated on the right *y*-axis. In the AMR section, *aadA2*, and *aac(6′)-Ib-cr* confer resistance to aminoglycosides, while $bla_{\text{CTX-M-15}}$ confers resistance to beta-lactam antibiotics, particularly third-generation cephalosporins; $bla_{\text{OXA-1}}$ provides resistance against beta-lactam antibiotics, including penicillins and some narrow-spectrum cephalosporins. The *dfrA14* confers resistance to trimethoprim, while the *fosA* gene and the *uhpT_E35Q* gene variant confer resistance to fosfomycin. *gyrA* and *parC* gene variants are associated with resistance to fluoroquinolones. *ompK35/36* porin variants are associated with a rise in the MIC for carbapenems, while *pmrB/mgrB* gene variants provide resistance against colistin. The chromosomal genes/mutations bar at the bottom refers to AMR determinants on the chromosome, the accessory plasmid bar refers to plasmids distinct from the pESBL-PH-2018-like plasmid carrying a carbapenemase gene, while the AMR genes on the ESBL plasmid bar refer to resistance genes located on plasmids similar to pESBL-PH-2018.

4. Discussion

Multiple lines of evidence demonstrate the widespread dissemination of an pESBL-PH-2018-like plasmid. These include a high Mash similarity, high coverage and nucleotide identity, and a low SNP difference in the core genetic loci of query plasmids. Similar plasmids also carried either identical or a similar number of the same AMR genes, alongside an identical plasmid replicon, heavy metal resistance genes, and conjugative transfer genes. The broad-host range of CTX-M-15-encoding plasmids has been previously recorded [11,14]. In addition, expansion of different bacterial clones harboring a similar CTX-M-15 encoding plasmid has been reported [33,34]. pESBL-PH-2018 may represent another plasmid, which can transfer between hosts. Once transferred, clonal expansion within receptive hosts can occur.

Plasmids similar to pESBL-PH-2018 were identified from 2012 to 2023, further confirming the long-term persistence of a pESBL-PH-2018-like plasmid. High conjugation efficiency has previously been reported for CTX-M-15-encoding plasmids, with high conjugation frequencies in the order of 10^{-1} recorded [35]. Together, the presence of similar plasmids in distinct hosts, alongside the identification of conjugative transfer genes, may indicate that horizontal gene transfer (HGT) could be responsible for the widespread dissemination of a pESBL-PH-2018-like plasmid. However, separate conjugation assays are required to determine the conjugative frequency for pESBL-PH-2018 and similar plasmids. Plasmid transfer efficiency can be highly variable depending on numerous factors, including the recipient strain, environmental conditions, selective pressures, and plasmid compatibility. These factors should be explored in future work.

The AMR region varied between the plasmids. Notably, the aminoglycoside resistance gene *aac(3)-IIe* was absent on a number of plasmids and may have been lost via IS*26*-mediated deletion, as the strains lacked both the resistance gene and IS*26* (such as pKPN342-1). For two plasmids, pMB6013_1 and pINF277.2, the copy number of the ESBL gene $bla_{\text{CTX-M-15,}}$ alongside other AMR genes, was repeated three times in a tandem array. Rolling Circle Replication (RCR) involves the amplification of DNA through the continuous replication of a translocatable unit (TU) formed by IS*26*. IS*26* mediates the excision of a DNA segment containing resistance genes, generating a circular TU. During RCR, DNA polymerase initiates replication at a nicked site, producing a long single-stranded DNA (ssDNA) tail, which is later converted into double-stranded DNA (dsDNA). Multiple copies of the TU are created rapidly, and IS*26* facilitates their reintegration into the plasmid, resulting in the tandem duplication of resistance genes. For plasmids pINF277.1 and pMB6013_1, IS*26*-mediated TU formation and RCR may have contributed to the amplification of resistance genes including $bla_{\text{CTX-M-15}}$, enhancing resistance and promoting their persistence and dissemination. Tobramycin selection pressure has been shown to lead to the duplication of the *aphA1* kanamycin and neomycin resistance gene from an *Acinetobacter baumannii* clinical strain MRSN56, due to IS*26*-mediated TU formation [36]. The AMR region of pESBL-PH-2018 may be subject to rearrangements and resistance gene duplications due to the presence of IS*26*, combined with antibiotic selection pressure, which is often encountered in clinical settings. Concerningly, for both plasmids with tandem repeats of AMR genes, dual β-lactamase-encoding genes, $bla_{\text{CTX-M-15}}$ and $bla_{\text{OXA-1,}}$ were identified. IS*26*-mediated co-amplification of two β-lactamase-encoding genes can yield a phenotype which is often non-susceptible to carbapenems, such as meropenem or ertapenem [37].

Beyond the presence of AMR and virulence genes present on the pESBL-PH-2018-like plasmid, the genotypic background of these strains was investigated to identify additional resistant/virulence-linked determinants associated with carbapenem and colistin resistance. A proportion of the strains carried the chromosomal integrative and conjugative element ICE*Kp* encoding the ABC transporter YbtPQ. Recently, the YbtPQ transporter has

been shown to reduce bacterial susceptibility to several classes of antibiotics, including carbapenems, likely mediated via broad range antimicrobial export [38]. The co-presence of carbapenemase genes in 7/8 of the strains encoding YbtPQ may increase the minimum inhibitory concentration (MIC) for carbapenems and other classes of antibiotics while contributing towards enhanced virulence via iron acquisition.

Furthermore, disruptions in the outer membrane porin gene *ompK36*, in concert with the presence of β-lactamase genes, have been linked with the development of non-carbapenemase-producing carbapenem-resistant Enterobacterales (non-CP-CRE). For example, a non-CP-CRE *K. pneumoniae* isolate, MB101, carried tandem amplification of a TU carrying $bla_{\text{OXA-1,}}$ together with an IS*Ecp1* transposition unit inserted into *ompK36* [39]. Six strains carried *ompK36* truncations without the presence of either chromosomal or plasmid carbapenem resistant genes. Notably, in two strains, multiple plasmid $bla_{\text{CTX-M-15}}$ genes were detected with either *ompK36* truncations (strain 3221, chromosomal accession: NZ_CP103635.1) or *ompK35* (strain U-KP1402, chromosomal accession: CP158302.1), yielding a potential non-CPE genotype. These two strains, and the other four strains with a single $bla_{\text{CTX-M-15}}$ copy, may have a background primed for the development of carbapenem resistance, a worrying scenario, given the presence of CTX determinants, which already confer resistance to cephalosporins, and other strains which already carried carbapenem resistant genes on separate plasmids. Such strains will be harder to treat and may present more opportunities for onward ESBL plasmid dissemination.

Low levels of antibiotics or heavy metals in polluted environments, or resulting from antibiotic consumption, can promote the selection and enrichment of MDR plasmid carriage among bacteria. Notably, very low concentrations of individual antibiotics, heavy metals, or their combinations can select for the large 220 kbp MDR plasmid, pUUH239.2, which confers resistance to aminoglycosides, β-lactams, tetracycline, macrolides, trimethoprim, sulfonamide, silver, copper, and arsenic [40]. Both antibiotics and heavy metals at sub-minimum inhibitory concentrations (sub-MICs) can select for pUUH239.2. For instance, the minimum selective concentration (MSC) for tetracycline is 17-fold lower, while for arsenite, it is approximately 140-fold lower than the corresponding MICs [40].

Areas affected by human pharmaceutical use may promote the maintenance and enrichment of MDR plasmids, contributing to their persistence and dissemination. This is particularly concerning for ESBL-encoding plasmids such as pESBL-PH-2018-like plasmids, which often encode resistance to both antimicrobials and heavy metals. In European surface waters, trimethoprim has been detected at concentrations reaching several hundred ng/L [41]—levels that exceed the MSC for trimethoprim.

While antibiotic and heavy metals may contribute towards the selection of MDR plasmids, non-native strains harboring MDR plasmids may be outcompeted in environmental settings. MDR plasmids are infrequently found in environmental settings such as stream and river water due to the competitive exclusion exerted by the native microbiota. A recent study demonstrated that both clinical and environmental ST147 *K. pneumoniae* strains carrying $bla_{\text{KPC-3}}$ on an IncN plasmid rapidly declined in urban runoff water due to competition from indigenous microbial communities [42]. The abundance of the $bla_{\text{KPC-3}}$ gene decreased significantly over time, correlating with the loss of cultivable *K. pneumoniae* rather than gene loss, indicating that host cell death was the primary cause of reduction. Additionally, the rise in Alphaproteobacteria abundance over time suggested that these bacteria may be particularly effective competitors against invasive species. In contrast, when incubated in sterile ultra-pure water (UP), where native microbiota were absent, the ST147 *K. pneumoniae* strains maintained viability and plasmid stability over eight days [42]. This highlights that in natural environments, where microbial diversity is high and resources

are limited, non-native *K. pneumoniae* carrying MDR plasmids, such as pESBL-PH-2018, are at a competitive disadvantage.

Using the strict thresholds set, we identified plasmids similar to pESBL-PH-2018, detected during a nosocomial outbreak in the United Kingdom. The strict thresholds applied, however, may underestimate the true prevalence of the ESBL-encoding plasmid. For example, we recently identified an ESBL-encoding plasmid, pEBM1, which underwent co-integrate formation with another $bla_{\text{CTX-M-15}}$-encoding plasmid from a *K. pneumoniae* strain [43]. A plasmid co-integrate may not be recognized as highly similar using the similarity thresholds. Our approach was designed to detect very similar plasmids, with a similar number of AMR genes; only four plasmids detected were missing four or fewer AMR genes from the 11 present on pESBL-PH-2018. However, despite this, the strict thresholds applied, definitively prove that plasmids very closely related to pESBL-PH-2018 have a wide host range, including across bacterial genera and species and display remarkable conservation over a 10-year period, existing in diverse strains with an extensive drug-resistant profile.

5. Conclusions

A plasmid identified from an outbreak strain of *K. pneumoniae* ST628 was structurally similar to plasmids identified in phylogenetically distinct *K. pneumoniae* hosts strains. The plasmid was also identified in different *Klebsiella* genera and *E.coli*. Similar plasmids across distinct strains suggest that the plasmid may disseminate via horizontal plasmid transfer into recipient hosts. Expansion in these hosts indicates the plasmid imposes a limited fitness burden. Furthermore, the combination of AMR genes with IS*26* may provide an environment whereby the copy number of ESBL genes can amplify, as detected in two strains here. Finally, the ESBL-encoding plasmid was identified in a background of AMR and virulence determinants. Importantly, in addition to ESBL plasmid carriage, truncations in the porin *ompK36* and the presence of the AMR export pump YbtPQ may lead to the development of non-carbapenemase-producing (NCP) carbapenem-resistant strains, which may become increasingly difficult to treat. Surveillance of pESBL-PH-2018-like plasmids is recommended to monitor further plasmid dissemination. This is a critical task, as current surveillance efforts mainly consider clonal expansion of resistance-encoding strains.

Supplementary Materials: The following supporting information can be downloaded at: https://www.mdpi.com/article/10.3390/microbiolres16050090/s1.

Author Contributions: Conceptualization, S.M.E.F.; methodology, S.M.E.F.; data curation, S.M.E.F.; formal analysis, S.M.E.F.; validation, S.M.E.F.; visualization, S.M.E.F.; writing—original draft preparation, S.M.E.F.; funding acquisition, A.M. and E.S.; supervision, A.M. and E.S.; writing—review and editing, resources; A.M. and E.S. All authors have read and agreed to the published version of the manuscript.

Funding: This research was funded by the Pfizer Global Medical Grant, grant number 68198087.

Institutional Review Board Statement: This study was conducted according to the guidelines of the Declaration of Helsinki and approved by the Ethics Committee of Bournemouth University (protocol code project ID 27771, on 13 March 2024).

Informed Consent Statement: Not applicable.

Data Availability Statement: Long- and short-read data for strain UHD-2018, including pESBL-PH-2018, can be found on the Sequence Read Archive (SRA) on NCBI under the Bioproject accession number PRJNA1150551, https://www.ncbi.nlm.nih.gov/sra/?term=PRJNA1150551 (accessed 21 August 2024). UHD-2018 chromosome accession: CP168069.1, plasmid pESBL-PH-2018 accession: CP168070.1.

Conflicts of Interest: The authors declare no conflicts of interest.

References

1. Chapelle, C.; Gaborit, B.; Dumont, R.; Dinh, A.; Vallée, M. Treatment of UTIs due to *Klebsiella pneumoniae* carbapenemase-producers: How to use new antibiotic drugs? A narrative review. *Antibiotics* **2021**, *10*, 1332. [CrossRef] [PubMed]
2. Lester, R.; Musicha, P.; Kawaza, K.; Langton, J.; Mango, J.; Mangochi, H.; Bakali, W.; Pearse, O.; Mallewa, J.; Denis, B.; et al. Effect of resistance to third-generation cephalosporins on morbidity and mortality from bloodstream infections in Blantyre, Malawi: A prospective cohort study. *Lancet Microbe* **2022**, *3*, e922–e930. [CrossRef]
3. Rozenkiewicz, D.; Esteve-Palau, E.; Arenas-Miras, M.; Grau, S.; Duran, X.; Sorlí, L.; Montero, M.M.; Horcajada, J.P. Clinical and economic impact of community-onset urinary tract infections caused by ESBL-producing *Klebsiella pneumoniae* requiring hospitalization in Spain: An observational cohort study. *Antibiotics* **2021**, *10*, 585. [CrossRef] [PubMed]
4. World Health Organisation. Global Priority List of Antibiotic-Resistant Bacteria to Guide Research, Discovery, and Development of New Antibiotics. Available online: https://www.who.int/publications/i/item/9789240093461 (accessed on 14 May 2024).
5. Fostervold, A.; Raffelsberger, N.; Hetland, M.A.; Bakksjø, R.; Bernhoff, E.; Samuelsen, Ø.; Sundsfjord, A.; Afset, J.E.; Berntsen, C.F.; Bævre-Jensen, R.; et al. Risk of death in *Klebsiella pneumoniae* bloodstream infections is associated with specific phylogenetic lineages. *J. Infect.* **2024**, *88*, 106155. [CrossRef]
6. Yang, X.; Man, M.Y.; Heng, H.; Chan, B.K.W.; Hu, Q.; Chan, E.W.C.; Shum, H.P.; Chen, S. Molecular epidemiology and clinical impact of *Klebsiella* spp. causing bloodstream infections in Hong Kong. *EBioMedicine* **2024**, *101*, 104998. [CrossRef]
7. Murray, C.J.; Ikuta, K.S.; Sharara, F.; Swetschinski, L.; Aguilar, G.R.; Gray, A.; Han, C.; Bisignano, C.; Rao, P.; Wool, E.; et al. Global burden of bacterial antimicrobial resistance in 2019: A systematic analysis. *Lancet* **2022**, *399*, 629–655. [CrossRef] [PubMed]
8. Poulou, A.; Voulgari, E.; Vrioni, G.; Koumaki, V.; Xidopoulos, G.; Chatzipantazi, V.; Markou, F.; Tsakris, A. Outbreak caused by an ertapenem-resistant, CTX-M-15-Producing *Klebsiella pneumoniae* sequence type 101 clone carrying an OmpK36 Porin variant. *J. Clin. Microbiol.* **2013**, *51*, 3176–3182. [CrossRef]
9. Zhou, K.; Lokate, M.; Deurenberg, R.H.; Arends, J.; Lo-Ten Foe, J.; Grundmann, H.; Rossen, J.W.; Friedrich, A.W. Characterization of a CTX-M-15 producing *Klebsiella pneumoniae* outbreak strain assigned to a novel sequence type (1427). *Front. Microbiol.* **2015**, *6*, 1250. [CrossRef]
10. Heiden, S.E.; Hübner, N.; Bohnert, J.A.; Heidecke, C.; Kramer, A.; Balau, V.; Gierer, W.; Schaefer, S.; Eckmanns, T.; Gatermann, S.; et al. A *Klebsiella pneumoniae* ST307 outbreak clone from Germany demonstrates features of extensive drug resistance, hypermucoviscosity, and enhanced iron acquisition. *Genome Med.* **2020**, *12*, 113. [CrossRef]
11. Wyres, K.L.; Hawkey, J.; Hetland, M.A.; Fostervold, A.; Wick, R.R.; Judd, L.M.; Hamidian, M.; Howden, B.P.; Löhr, I.H.; Holt, K.E. Emergence and rapid global dissemination of CTX-M-15-associated *Klebsiella pneumoniae* strain ST307. *J. Antimicrob. Chemother.* **2019**, *74*, 577–581. [CrossRef]
12. Emeraud, C.; Figueiredo, S.; Bonnin, R.A.; Khecharem, M.; Ouzani, S.; Leblanc, P.; Jousset, A.B.; Fortineau, N.; Duranteau, J.; Dortet, L. Outbreak of CTX-M-15 extended-spectrum β-lactamase-Producing *Klebsiella pneumoniae* ST394 in a French intensive care unit dedicated to COVID-19. *Pathogens* **2021**, *10*, 1426. [CrossRef]
13. Dolejska, M.; Brhelova, E.; Dobiasova, H.; Krivdova, J.; Jurankova, J.; Sevcikova, A.; Dubska, L.; Literak, I.; Cizek, A.; Vavrina, M.; et al. Dissemination of IncFIIK-type plasmids in multiresistant CTX-M-15-producing Enterobacteriaceae isolates from children in hospital paediatric oncology wards. *Int. J. Antimicrob. Agents* **2012**, *40*, 510–515. [CrossRef] [PubMed]
14. Pedersen, T.; Tellevik, M.G.; Kommedal, Ø.; Lindemann, P.C.; Moyo, S.J.; Janice, J.; Blomberg, B.; Samuelsen, Ø.; Langeland, N. Horizontal plasmid transfer among *Klebsiella pneumoniae* isolates is the key factor for dissemination of extended-spectrum β-lactamases among children in Tanzania. *mSphere* **2020**, *5*, e00428-20. [CrossRef]
15. Fordham, S.M.; Drobniewski, F.; Barrow, M.; Hutchings, M.; Crowther, K.; Richards, D.; Bolton, P.; Mantzouratou, A.; Sheridan, E. Genetic analyses of rare ESBL ST628 *Klebsiella pneumoniae* detected during a protracted nosocomial outbreak in the United Kingdom. *Microorganisms* **2024**, *12*, 883. [CrossRef] [PubMed]
16. Chen, S. Ultrafast one-pass FASTQ data preprocessing, quality control, and deduplication using fastp. *iMeta* **2023**, *2*, e107. [CrossRef] [PubMed]
17. De Coster, W.; D'Hert, S.; Schultz, D.T.; Cruts, M.; Van Broeckhoven, C. NanoPack: Visualizing and processing long-read sequencing data. *Bioinformatics* **2018**, *34*, 2666–2669. [CrossRef]
18. Wick, R.R.; Judd, L.M.; Cerdeira, L.T.; Hawkey, J.; Méric, G.; Vezina, B.; Wyres, K.L.; Holt, K.E. Trycycler: Consensus long-read assemblies for bacterial genomes. *Genome Biol.* **2021**, *22*, 266. [CrossRef]
19. Kolmogorov, M.; Yuan, J.; Lin, Y.; Pevzner, P.A. Assembly of long, error-prone reads using repeat graphs. *Nat. Biotechnol.* **2019**, *37*, 540–546. [CrossRef]
20. Wick, R.R.; Holt, K.E. Benchmarking of long-read assemblers for prokaryote whole genome sequencing. *F1000Research* **2021**, *8*, 2138. [CrossRef]
21. Vaser, R.; Šikić, M. Time- and memory-efficient genome assembly with Raven. *Nat. Comput. Sci.* **2021**, *1*, 332–336. [CrossRef]

22. Bouras, G.; Judd, L.M.; Edwards, R.A.; Vreugde, S.; Stinear, T.P.; Wick, R.R. How low can you go? Short-read polishing of Oxford Nanopore bacterial genome assemblies. *Microb. Genom.* **2024**, *10*, 001254. [CrossRef] [PubMed]
23. Ondov, B.D.; Treangen, T.J.; Melsted, P.; Mallonee, A.B.; Bergman, N.H.; Koren, S.; Phillippy, A.M. Mash: Fast genome and metagenome distance estimation using MinHash. *Genome Biol.* **2016**, *17*, 132. [CrossRef]
24. Hawkey, J.; Wyres, K.L.; Judd, L.M.; Harshegyi, T.; Blakeway, L.; Wick, R.R.; Jenney, A.W.; Holt, K.E. ESBL plasmids in *Klebsiella pneumoniae*: Diversity, transmission and contribution to infection burden in the hospital setting. *Genome Med.* **2022**, *14*, 97. [CrossRef] [PubMed]
25. Feldgarden, M.; Brover, V.; Gonzalez-Escalona, N.; Frye, J.G.; Haendiges, J.; Haft, D.H.; Hoffmann, M.; Pettengill, J.B.; Prasad, A.B.; Tillman, G.E.; et al. AMRFinderPlus and the reference gene catalog facilitate examination of the genomic links among antimicrobial resistance, stress response, and virulence. *Sci. Rep.* **2021**, *11*, 12728. [CrossRef]
26. Schwengers, O.; Jelonek, L.; Dieckmann, M.A.; Beyvers, S.; Blom, J.; Goesmann, A. Bakta: Rapid and standardized annotation of bacterial genomes via alignment-free sequence identification. *Microb. Genom.* **2021**, *7*, 000685. [PubMed]
27. Che, Y.; Yang, Y.; Xu, X.; Břinda, K.; Polz, M.F.; Hanage, W.P.; Zhang, T. Conjugative plasmids interact with insertion sequences to shape the horizontal transfer of antimicrobial resistance genes. *Proc. Natl. Acad. Sci. USA* **2021**, *118*, e2008731118. [CrossRef]
28. Croucher, N.J.; Page, A.J.; Connor, T.R.; Delaney, A.J.; Keane, J.A.; Bentley, S.D.; Parkhill, J.; Harris, S.R. Rapid phylogenetic analysis of large samples of recombinant bacterial whole genome sequences using Gubbins. *Nucleic Acids Res.* **2014**, *43*, e15. [CrossRef]
29. Evans, D.; Sundermann, A.; Griffith, M.; Rangachar Srinivasa, V.; Mustapha, M.; Chen, J.; Dubrawski, A.; Cooper, V.; Harrison, L.; Van Tyne, D. Empirically derived sequence similarity thresholds to study the genomic epidemiology of plasmids shared among healthcare-associated bacterial pathogens. *eBioMedicine* **2023**, *93*, 104681. [CrossRef]
30. Page, A.J.; Cummins, C.A.; Hunt, M.; Wong, V.K.; Reuter, S.; Holden, M.T.; Fookes, M.; Falush, D.; Keane, J.A.; Parkhill, J. Roary: Rapid large-scale prokaryote pan genome analysis. *Bioinformatics* **2015**, *31*, 3691–3693. [CrossRef]
31. Alikhan, N.; Petty, N.K.; Zakour, N.L.B.; Beatson, S.A. BLAST Ring Image Generator (BRIG): Simple prokaryote genome comparisons. *BMC Genom.* **2011**, *12*, 402. [CrossRef]
32. Wong, J.L.C.; Romano, M.; Kerry, L.E.; Kwong, H.; Low, W.; Brett, S.J.; Clements, A.; Beis, K.; Frankel, G. OmpK36-mediated Carbapenem resistance attenuates ST258 *Klebsiella pneumoniae* in vivo. *Nat. Commun.* **2019**, *10*, 3957. [CrossRef] [PubMed]
33. Negeri, A.A.; Mamo, H.; Gahlot, D.K.; Gurung, J.M.; Seyoum, E.T.; Francis, M.S. Characterization of plasmids carrying $bla_{\text{CTX-M}}$ genes among extra-intestinal *Escherichia coli* clinical isolates in Ethiopia. *Sci. Rep.* **2023**, *13*, 8595. [CrossRef]
34. Wranne, M.S.; Karami, N.; Sriram, K.K.; Jaén-Luchoro, D.; Yazdanshenas, S.; Lin, Y.; Kabbinale, A.; Flach, C.; Westerlund, F.; Åhrén, C. Author correction: Comparison of CTX-M encoding plasmids present during the early phase of the ESBL pandemic in western Sweden. *Sci. Rep.* **2024**, *14*, 16678. [CrossRef] [PubMed]
35. Minja, C.A.; Shirima, G.; Mshana, S.E. Conjugative plasmids disseminating CTX-M-15 among human, animals and the environment in Mwanza Tanzania: A need to intensify one health approach. *Antibiotics* **2021**, *10*, 836. [CrossRef] [PubMed]
36. Harmer, C.J.; Lebreton, F.; Stam, J.; McGann, P.T.; Hall, R.M. Mechanisms of IS*26*-Mediated Amplification of the *aphA1* Gene Leading to Tobramycin Resistance in an *Acinetobacter baumannii* Isolate. *Microbiol. Spectr.* **2022**, *10*, e02287-22. [CrossRef]
37. Shropshire, W.C.; Konovalova, A.; McDaneld, P.; Gohel, M.; Strope, B.; Sahasrabhojane, P.; Tran, C.N.; Greenberg, D.; Kim, J.; Zhan, X.; et al. Systematic analysis of mobile genetic elements mediating β-lactamase gene amplification in noncarbapenemase-producing carbapenem-resistant *Enterobacterales* bloodstream infections. *mSystems* **2022**, *7*, e00476-22. [CrossRef]
38. Farzand, R.; Rajakumar, K.; Barer, M.R.; Freestone, P.P.; Mukamolova, G.V.; Oggioni, M.R.; O'Hare, H.M. A virulence associated Siderophore importer reduces antimicrobial susceptibility of *Klebsiella pneumoniae*. *Front. Microbiol.* **2021**, *12*, 607512. [CrossRef]
39. Shropshire, W.C.; Aitken, S.L.; Pifer, R.; Kim, J.; Bhatti, M.M.; Li, X.; Kalia, A.; Galloway-Peña, J.; Sahasrabhojane, P.; Arias, C.A.; et al. IS*26*-mediated amplification of $bla_{\text{OXA-1}}$ and $bla_{\text{CTX-M-15}}$ with concurrent outer membrane Porin disruption associated with de novo carbapenem resistance in a recurrent bacteraemia cohort. *J. Antimicrob. Chemother.* **2020**, *76*, 385–395. [CrossRef]
40. Gullberg, E.; Albrecht, L.M.; Karlsson, C.; Sandegren, L.; Andersson, D.I. Selection of a Multidrug resistance plasmid by sublethal levels of antibiotics and heavy metals. *mBio* **2014**, *5*, e01918-14. [CrossRef]
41. Straub, J. An environmental Risk Assessment for Human-Use Trimethoprim in European surface waters. *Antibiotics* **2013**, *2*, 115–162. [CrossRef]
42. Ferreira, C.; Luzietti, L.; Ribeirinho-Soares, S.; Nunes, O.C.; Vaz-Moreira, I.; Manaia, C.M. Survival of clinical and environmental carbapenem-resistant *Klebsiella pneumoniae* ST147 in surface water. *Environ. Res.* **2023**, *237*, 116928. [CrossRef] [PubMed]
43. Fordham, S.M.E.; Barrow, M.; Mantzouratou, A.; Sheridan, E. Genomic analyses of an *Escherichia coli* and *Klebsiella pneumoniae* urinary tract co-infection using long-read nanopore sequencing. *Microbiologyopen* **2024**, *13*, e1396. [CrossRef]